Accepted Manuscript

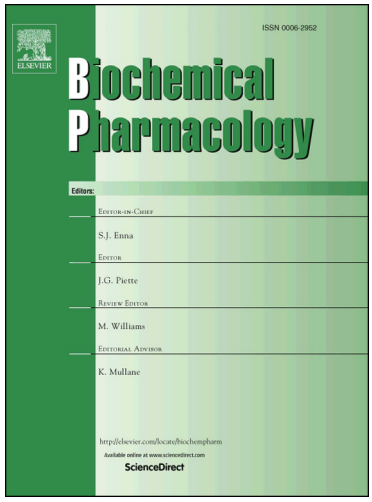


Inhibitory effects of drugs on the metabolic activity of mouse and human aldehyde oxidases and influence on drug–drug interactions

Naoki Takaoka, Seigo Sanoh, Katsuhiro Okuda, Yaichiro Kotake, Go Sugahara, Ami Yanagi, Yuji Ishida, Chise Tateno, Yoshitaka Tayama, Kazumi Sugihara, Shigeyuki Kitamura, Mami Kurosaki, Mineko Terao, Enrico Garattini, Shigeru Ohta

PII: S0006-2952(18)30160-6
DOI: https://doi.org/10.1016/j.bcp.2018.04.017
Reference: BCP 13126

To appear in: *Biochemical Pharmacology*

Received Date: 6 February 2018
Accepted Date: 16 April 2018

Please cite this article as: N. Takaoka, S. Sanoh, K. Okuda, Y. Kotake, G. Sugahara, A. Yanagi, Y. Ishida, C. Tateno, Y. Tayama, K. Sugihara, S. Kitamura, M. Kurosaki, M. Terao, E. Garattini, S. Ohta, Inhibitory effects of drugs on the metabolic activity of mouse and human aldehyde oxidases and influence on drug–drug interactions, *Biochemical Pharmacology* (2018), doi: https://doi.org/10.1016/j.bcp.2018.04.017

# Inhibitory effects of drugs on the metabolic activity of mouse and human aldehyde oxidases and influence on drug–drug interactions

Naoki Takaoka[1], Seigo Sanoh[1], Katsuhiro Okuda[2], Yaichiro Kotake[1], Go Sugahara[3], Ami Yanagi[3], Yuji Ishida[3,4], Chise Tateno[3,4], Yoshitaka Tayama[5], Kazumi Sugihara[5], Shigeyuki Kitamura[6], Mami Kurosaki[7], Mineko Terao[7], Enrico Garattini[7], Shigeru Ohta[1]

[1]Graduate School of Biomedical and Health Sciences, Hiroshima University

[2]Asahikawa Medical University

[3]R&D Dept., PhoenixBio, Co., Ltd

[4]Research Center for Hepatology and Gastroenterology, Hiroshima University

[5]Faculty of Pharmaceutical Sciences, Hiroshima International University

[6]Nihon Pharmaceutical University

[7]Laboratory of Molecular Biology, Institute di Ricerche Farmacologie “Mario Negri”

*Corresponding author. E-mail address: sanoh@hiroshima-u.ac.jp

## Running title

Species differences of drugs in aldehyde oxidase inhibition

## Abbreviations

AOX, aldehyde oxidase; AUC, area under the plasma concentration time curve; CYP, cytochrome P450; DDI, drug−drug interaction; LC, liquid chromatography; MBE, minimum binding energy; MS/MS, tandem mass spectrometry; ESI, electrospray ionization; PK, pharmacokinetics; RI, replacement index; S9, 9,000×g supernatant; TET, tetracycline.

**Abstract**

As aldehyde oxidase (AOX) plays an emerging role in drug metabolism, understanding its significance for drug–drug interactions (DDI) is important. Therefore, we tested 10 compounds for species-specific and substrate-dependent differences in the inhibitory effect of AOX activity using genetically engineered HEK293 cells over-expressing human AOX1, mouse AOX1 or mouse AOX3. The $IC_{50}$ values of 10 potential inhibitors of the three AOX enzymes were determined using phthalazine and $O^6$-benzylguanine as substrates. 17β-Estradiol, menadione, norharmane and raloxifene exhibited marked differences in inhibitory effects between the human and mouse AOX isoforms when the phthalazine substrate was used. Some of the compounds tested exhibited substrate-dependent differences in their inhibitory effects. Docking simulations with human AOX1 and mouse AOX3 were conducted for six representative inhibitors. The rank order of the minimum binding energy reflected the order of the corresponding $IC_{50}$ values. We also evaluated the potential DDI between an AOX substrate ($O^6$-benzylguanine) and an inhibitor (hydralazine) using chimeric mice with humanized livers. Pretreatment of hydralazine increased the maximum plasma concentration ($C_{max}$) and the area under the plasma concentration-time curve ($AUC_{0–24}$) of $O^6$-benzylguanine compared to single administration. Our *in vitro* data indicate species-specific and substrate-dependent differences in the inhibitory effects on AOX

activity. Our *in vivo* data demonstrate the existence of a DDI which may be of relevance in the clinical context.

**Keywords** : aldehyde oxidase, drug–drug interaction, inhibition, species differences, chimeric mice with humanized liver

## 1. Introduction

Mammalian aldehyde oxidases (AOXs) are cytosolic molybdoflavoprotein which acts as homodimers consisting of two identical 150-kDa subunits. AOXs play a key role in drug metabolism because of their broad substrate selectivity, as they oxidize a wide variety of aldehydes and heterocyclic aromatic compounds [1,2]. Among the known substrates of mammalian AOXs, aza-heterocyclic aromatic compounds are of particular interest in drug development because medicinal chemists frequently introduce these ring systems into chemical scaffolds to improve solubility and lower lipophilicity. This is likely to reduce metabolism by cytochrome P450 enzymes [3–5]. The strategy ultimately resulted in alternative metabolic clearance mechanisms mediated by other enzymes, including human AOX1 [6,7]. In fact, a recent review article indicates that numerous authorized drugs (13%) or drug candidates (approximately 45%) could be AOX substrates on the basis of their chemical structures [8].

AOXs exhibit profound species-specific differences in terms of protein expression and enzymatic activity [7,9,10]. AOXs are widely expressed in various species from bacteria to humans. In mammals, four AOX isoforms (AOX1, AOX2, AOX3 and AOX4), which are expressed in a tissue-specific manner, have been identified [11,12]. Regarding the liver, the most important organ in terms of drug metabolism, the expression profile of AOXs differs between humans and other animal species. Only *AOX1* is expressed in the human and

monkey hepatic tissue, whereas *AOX1* and *AOX3* are expressed in rodent liver and no AOX isoform is present in dog liver [10]. Mouse AOX1 is an ortholog of human AOX1 and the overall level of their amino acid identity is 83%. In particular, the 85 kDa carboxyl terminal regions of the two proteins, which contain the substrate binding pocket, show a level of similarity close to 84%. As for mouse AOX3, the overall level of amino acid identity with both mouse and human AOX1 is approximately 61%, which increases to 62% if the regions containing the substrate binding pockets are considered [2,12].

As the major isoform expressed in rodent liver is *AOX3* followed by *AOX1* [13], the quantitative enzymatic activity of AOX differs in humans and rodents. Numerous reports based on *in vitro* models have demonstrated differences in liver AOX activity against various substrates between humans and experimental animals [9,14]. In addition, recent studies have indicated that some promising drug candidates have been discontinued in phase 1 clinical trials due to unpredicted and extensive AOX metabolism in humans [7,15]. The remarkable species-specific differences in AOX protein expression and activity are a major problem in pre-clinical drug-development.

Human AOX1 is inhibited by numerous compounds including drugs and diet-derived constituents. Obach et al. (2004) screened a library of 239 drugs and xenobiotics for potential inhibition of human AOX1 using phthalazine as a substrate. Of these 239 compounds, 36 inhibited enzymatic activity by ≥80% at a concentration of 50 μM [16]. Furthermore,

hydralazine has been shown to be an inhibitor of AOX activity in rabbit, guinea pig, baboon, and human liver [17–19]. In addition to drugs, diet-derived constituents were also reported to inhibit AOX activity (e.g., epicatechin gallate and epigallocatechin gallate) [20,21]. In this context, an interesting compound is represented by norharmane, which exhibits an isoform-specific inhibitory effect on *AOX3* in mouse liver [13].

Only one study evaluated species-specific differences in AOX inhibitory effects using cytosolic fractions from the livers of humans and experimental animals [14]. However, as mentioned above, the AOX isoforms expressed in the liver of humans and many experimental animals are different. Therefore, to obtain a deeper understanding of species-specific differences in inhibitory effects, we generated HEK293 cells conditionally over-expressing human AOX1, mouse AOX1 or mouse AOX3. Using this system, we conducted comparative *in vitro* studies with couples of AOX substrates and inhibitors. These studies were complemented by *in silico* docking studies performed with selected AOX inhibitors. In addition, we performed *in vivo* drug-drug interactions (DDI) studies on the $O^6$-benzylguanine and hydralazine AOX substrate/inhibitor couple using chimeric mice with humanized livers. Kitamura et al. (2008) [22] suggested that aldehyde oxidase in the liver of chimeric mice is functionally a human-type aldehyde oxidase in $N^1$-methylnicotinamide metabolism. Furthermore, it is expected to be a good model for predicting human drug metabolism and pharmacokinetics (PK) mediated by AOX [23,24].

## 2. Materials and Methods

### *2.1. Chemicals and reagents*

Dulbecco's modified Eagle's medium (DMEM; supplemented with low glucose, GlutaMax, and pyruvate), Zeocin and tetracycline-free fetal bovine serum (FBS) were purchased from Thermo Fisher Scientific (Waltham, MA). Blasticidin S hydrochloride was purchased from Nacalai Tesque (Kyoto, Japan). Acetonitrile, clozapine, carbamazepine, 17β-estradiol, menadione, raloxifene, tetracycline hydrochloride and goat anti-rabbit IgG were purchased from Sigma-Aldrich (St. Louis, MO). Phthalazine, phthalazone, $O^6$-benzylguanine, amitriptyline, chlorpromazine, hydralazine, ketoconazole, norharmane, dimethyl sulfoxide (DMSO), hydrochloric acid and 0.5% methyl cellulose were purchased from Wako Pure Chemical Industries (Osaka, Japan). 8-oxo-$O^6$-Benzylguanine was purchased from Toronto Research Chemicals (Toronto, ON, Canada). Loratadine, methanol and 99% formic acid were purchased from Kanto Chemical (Tokyo, Japan).

### *2.2. Generation of the AOX expressing cell clones*

The cDNA coding for human AOX1 was amplified from chondrosarcoma RNA by nested PCR using the following oligonucleotides for the first round PCR: 5'-gttggtactttaggctccagcaagc-3' (nucleotides 171-195 of the cDNA published in MN_001159)

and 5'-agcatcttccagcacagagataggac-3' (nucleotides complementary to 4369-4394 in MN_001159). The second nested amplification step was performed with following oligonucleotides: 5'-tagcggccgcgcgcggacaccacaatggaccgggcgtccgagct-3' (nucleotides 285-318 in NM_001159, the underlined sequence is inserted to create a NotI recognition site) and 5'-tgctcgaggcactctgttttctccagaag-3'(nucleotides complementary to 4328-4347 in NM_001159, the underlined sequence is inserted to create a XhoI recognition site). The generated 4 kb fragment was subcloned in the NotI–XhoI site of pBluescript (Stratagene, San Diego, CA). Subsequently, the cDNA construct in Bluescript was digested with KpnI and Not I, and the resulting cDNA fragment was inserted in the KpnI-Not I digested pcDNA4/TO plasmid (Invitrogen, Carlsbad, CA). The nucleotide sequence of human AOX1 has been submitted to the GeneBank™/EBI Data Bank with accession number (MF667933). The cDNA clones coding for the mouse AOX1 and the mouse AOX3 were subcloned in the pcDNA4/TO plasmid [25]. HEK293 cells were stably transfected with pcDNA6/TR (Invitrogen, Carlsbad, CA) to create a cell line, *TR21* (Blasticidin S resistant), that expresses the tetracycline repressor in the absence of tetracycline in the growth medium. The cDNAs coding for human AOX1, mouse AOX1 and mouse AOX3 in pcDNA4/TO vector were transfected in *TR21* cells, and stably transfected cell clones were isolated in the presence of Zeocin. The tetracycline-dependent production of human AOX1, mouse AOX1 and mouse AOX3 proteins was confirmed by Western blot analysis, using specific antibodies as

previously described [13]. To demonstrate that the three proteins are expressed in a catalytically active form, we determined phthalazine oxidizing enzymatic activity using the Amplex Red xanthine/xanthine oxidase assay kit (Invitrogen, Carlsbad, CA).

### *2.3. Cell culture and induction of enzyme expression*

The expression of human AOX1, mouse AOX1 and mouse AOX3 was conducted using the HEK293 cell-derived TR21 cell line, stably transfected with plasmids containing human AOX1, mouse AOX1 or mouse AOX3 cDNA. In standard conditions, the doubling time of all the cell lines generated is approximately 2 days. The passage number used for the experiments was between 12 and 28. Each set of HEK293 cells was maintained at 37 °C in DMEM supplemented with 10 µg/mL blasticidin S hydrochloride, 50 µg/mL Zeocin, and 5% FBS. To induce the expression of each AOX isoform, the medium was replaced with the same medium with 1 µg/mL tetracycline hydrochloride. At 48 h after this treatment with tetracycline, each set of cells was harvested and suspended in 0.1 M Tris-HCl buffer (pH 7.5) for mouse AOX1 and mouse AOX3 or 0.1 M potassium phosphate buffer (pH 7.5) for human AOX1. Each cell suspension was subjected to cell disruption by freeze–thawing and centrifuged at 9000×g for 20 min. The supernatant (S9 fraction) was used for evaluation of enzymatic activity or inhibitory effects.

### *2.4. Evaluation of enzymatic activity and inhibitory effects*

Incubation mixtures consisted of substrates (phthalazine or $O^6$-benzylguanine), inhibitor (or vehicle for control without inhibitor), S9 fraction (final concentration of 1 mg protein/mL), and Tris-HCl buffer (0.1 M, pH 7.4). The mixtures were pre-incubated for 5 min at 37°C. Reactions were initiated by adding the solution of phthalazine or $O^6$-benzylguanine, yielding a final volume of 50 µL. The final acetonitrile concentration was <1% v/v. After incubation, reactions were terminated by adding methanol containing carbamazepine as an internal standard. The incubation time of phthalazine was 3 min for each isoform. The incubation times of $O^6$-benzylguanine were 20 and 60 min for human AOX1 and mouse AOX1, respectively. After centrifugation at 14,000×g for 5 min at 4°C, the aliquot of the supernatant was mixed with 0.1% formic acid. The mixture was analyzed for formed metabolites, phthalazone, or 8-oxo-$O^6$-benzylguanine by liquid chromatography–tandem mass spectroscopy (LC/MS/MS, see below). Under these experimental conditions, phthalazone or 8-oxo-$O^6$-benzylguanine formation linearly increased with respect to incubation time.

### *2.5. Saturation kinetics of phthalazine and $O^6$-benzylguanine*

Incubation proceeded as described above; the final concentrations of phthalazine and $O^6$-benzylguanine were in the ranges of 1–200 µM and 5–500 µM, respectively. Kinetic parameters ($K_m$, $V_{max}$) were obtained by fitting the Michaelis–Menten equation to

substrate-versus-velocity data via nonlinear least squares regression using GraphPad Prism (GraphPad Software, La Jolla, CA)

### *2.6. $IC_{50}$ determination for selected compounds*

Incubation proceeded as described above using phthalazine at concentrations of 60, 120 and 5 μM (for human AOX1, mouse AOX1 and mouse AOX3, respectively) or $O^6$-benzylguanine at 150 μM for human AOX1 and mouse AOX1, which approximated each $K_m$ value. Each test compound was added to a mixture before pre-incubation for 5 min at five predetermined concentrations. Relative AOX activity was expressed as the percent of the rate of metabolite formation in the presence of inhibitor to that in its absence. $IC_{50}$ values were obtained by a four-parameter logistic model using Prism 6 (GraphPad Software, La Jolla, CA).

### 2.7. *In silico docking study*

Energy-minimized ligand structures were constructed and optimized using ChemBio3D 14.0 (PerkinElmer Co., Ltd.). Structures of proteins (human AOX1 and mouse AOX3) were obtained from the solved crystal structure in the Protein Data Bank (PDB). The information of protein structures is as follows: human AOX1 (4UHW; 2.6 Å resolution) and mouse AOX3 (PDB ID 3ZYV; 2.55 Å resolution) [26,27]. Simulations regarding the

interaction between tested compound structures and human AOX1 or mouse AOX3 were performed using Autodock 4.2.6 [28]. We used the blind docking technique to evaluate the probable binding location of ligands in both proteins. The strategy of blind docking includes a search over the entire protein surface for binding sites. Lamarckian genetic algorithm was selected as the docking parameter. Compounds and nine selected amino acid residues in the active site were flexible during each simulation. The flexible amino acid residues were as follows: Gln 772, Val 807, Met 885, Lys 889, Phe 919, Lue 1014, Gly 1015, Ala 1019 and Glu 1266 for human AOX1 and Gln 772, Ala 807, Tyr 885, Lys 889, Phe 919, Phe 1014, Prp 1015, Tyr 1019 and Glu 1266 for mouse AOX3, expressed using mouse AOX3 numbering [26]. The other docking parameters of Autodock were kept at default values. After simulations, 100 conformations of compounds in complex with the active site in both AOX proteins were ranked on the basis of frequency and binding energy. The binding affinity of selected compounds was calculated by the program in terms of binding energy (kcal/mol).

### *2.8. In vivo DDI study in chimeric mice with humanized livers*

The present study was approved by the animal ethics committee and was conducted in accordance with the regulations on the use of living modified organisms of Phoenix Bio Co., Ltd. (Hiroshima, Japan) and Hiroshima University. Chimeric mice with humanized livers (male; 16–18 weeks of age), created by transplanting human hepatocytes to cDNA-uPA SCID

mice, were prepared by Phoenix Bio Co., Ltd. [29]. These mice were housed in a temperature- and humidity-controlled environment under a 12-h light/dark cycle with free access to tap water and food. The transplanted human hepatocytes were obtained from BD Biosciences (San Jose, CA). The replacement ratio of host hepatocytes with human hepatocytes, calculated as the replacement index (RI), was determined by measurement of the human albumin level in blood collected from each chimeric mouse [29]. The average RI value of chimeric mice used in this study was 95.4 ± 4.01% (mean ± SD).

$O^6$-Benzylguanine suspended solution and hydralazine solution (5 mL/kg) were orally administered to each group at 10 and 30 mg/kg body weight, respectively. $O^6$-Benzylguanine was suspended in 0.5% methyl cellulose with an amount of hydrochloric acid equivalent to that of $O^6$-benzylguanine. Hydralazine solution was formulated using hydralazine in 0.5% methyl cellulose and was orally administered 1 h prior to oral administration of $O^6$-benzylguanine. Blood samples were collected from the orbital vein of each chimeric mouse at 0.1, 0.25, 0.5, 1, 3 and 24 h after treatment with $O^6$-benzylguanine under isoflurane anesthesia. Plasma samples separated after centrifugation were stored at −30°C until analysis. After thawing, these plasma samples were mixed with methanol containing carbamazepine as an internal standard and 50% methanol. After centrifugation at 14,000 g for 5 min at 4°C, the aliquot of the supernatant was diluted with 0.1% formic acid. The mixture was analyzed for $O^6$-benzylguanine, its metabolite and hydralazine by

LC/MS/MS (see below). The maximum plasma concentration ($C_{max}$) and the time at which the maximum concentration was achieved ($t_{max}$) were determined from actual values. The area under the plasma concentration-time curve ($AUC_{0–24}$) was estimated from the time course using the trapezoidal method.

### *2.9.Quantitation by LC/MS/MS Phthalazine and phthalazone*

Aliquots were injected into the LC system (Agilent Technologies, Santa Clara, CA). The mobile phase conditions for phthalazine and phthalazone consisted of 0.1% formic acid (A) and methanol (B) through a YMC-Triant C18 column (5 µm, 50 × 2.1 mm; YMC Co., Ltd., Kyoto, Japan) at 40°C. In an *in vitro* metabolic analysis using amitriptyline, the Inertsil ODS-3 column (5 µm, 50 × 2.1 mm; GL Sciences Inc., Tokyo, Japan) was used. The flow rate was set at 0.2 mL/min. The starting condition for the LC gradient was 100:0 (A/B). The mobile phase composition was changed to 30:70 (A/B) at 0–5 min, and this ratio was maintained until 8 min. The gradient was then returned to 100:0 (A/B) linearly at 8–8.1 min, and the column was reequilibrated to the initial conditions at 8.1–11.5 min.

#### *2.9.1. $O^6$-benzylguanine, 8-oxo-$O^6$-benzylguanine, and hydralazine.*

Aliquots were injected into the LC system. The mobile phase conditions for $O^6$-benzylguanine and 8-oxo-$O^6$-benzylguanine consisted of 0.1% formic acid (A) and

methanol (B) through a YMC-Triant C18 column (5µm, 50 x 2.1 mm; YMC Co., Ltd.) at 40°C. In an *in vitro* metabolic analysis using amitriptyline, the Inertsil ODS-3 column (5 µm, 50 × 2.1 mm; GL Sciences Inc., Tokyo, Japan) was used. The flow rate was set at 0.2 mL/min. The starting condition for the LC gradient was 90:10 (A/B). From The mobile phase composition was changed to 30:70 (A/B) at 0–5 min, and this ratio was maintained until 8 min. The gradient was then returned to 90:10 (A/B) linearly at 8.0–8.1 min, and the column was re-equilibrated to the initial conditions at 8.1–11 min. In PK analysis using hydralazine, the mobile phase conditions were similar to those used for phthalazine.

***2.9.2. MS/MS conditions.***

The MS/MS experiments were conducted using API2000 LC-MS/MS systems (Applied Biosystems, Foster, CA). Monitored *m/z* values of the precursor and product ion for phthalazine, $O^6$-benzylguanine, their metabolites and hydralazine under ESI positive ionization were as follows: phthalazine *m/z* = 130.9 $[M+H]^+$ to 104.2, phthalazone *m/z* = 146.4 $[M+H]^+$ to 101.6, $O^6$-benzylguanine *m/z* = 242.0 $[M+H]^+$ to 90.6, 8-oxo-$O^6$-benzylguanine *m/z* = 258.0 $[M+H]^+$ to 90.7, hydralazine *m/z* = 160.9 $[M+H]^+$ to 88.7 and carbamazepine *m/z* = 237.1 $[M+H]^+$ to 193.9.

***2.10. Statistical analysis***

Statistical significance between two groups was determined by two-tailed Student's *t* test. A value of $p < 0.05$ was considered statistically significant.

## Results

### *3.1. Determination of phthalazine and $O^6$-benzylguanine oxidizing activity by human AOX1, mouse AOX1 and mouse AOX3*

We stably transfected human AOX1, mouse AOX1 and mouse AOX3 cDNA constructs controlled by a tetracycline (TET) dependent promoter in a HEK293 derived cell line genetically engineered for the expression of the TET-repressor. In this cellular system, expression of the three catalytically active enzymes is obtained after exposure to TET. Western blot analyses confirming the expression of the human AOX1, mouse AOX1 and mouse AOX3 proteins are shown in Fig. 1A. On TET induction, the three enzymes are expressed in a catalytically active form, as indicated by the results obtained with phthalazine as a substrate (Fig. 1B).

We performed enzyme kinetic studies using S9 fractions of the HEK293 cell extracts. We selected phthalazine and $O^6$-benzylguanine as substrates [18,30]. The oxidative reaction products of phthalazine and $O^6$-benzylguanine generated by the three AOXs and confirmed by mass-spectrometry are illustrated in Fig. 2. Fig. 3 shows the substrate saturation curve for phthalazine and $O^6$-benzylguanine oxidation. The saturation kinetic parameters were determined by nonlinear regression analysis using the Michaelis–Menten kinetic model. In

the case of phthalazine oxidation, human AOX1, mouse AOX1 and mouse AOX3 exhibited good fitness to the model. The same was true in the case of $O^6$-benzylguanine oxidation by human and mouse AOX1. In contrast, mouse AOX3 did not oxidize $O^6$-benzylguanine into 8-oxo-$O^6$-benzylguanine (data not shown). Table 1 lists the $K_m$ and $V_{max}$ values of the three enzymes expressed in HEK293 cells. These data indicate isoform-dependent differences in the oxidation of the two substrates by the three AOX enzymes.

### *3.2. Comparative inhibitory effects of selected compounds on the phthalazine oxidizing activity of human and mouse AOXs*

Among the compounds reported to act as AOX inhibitors [13,16,18], we selected 10 compounds (amitriptyline, chlorpromazine, clozapine, 17β-estradiol, hydralazine, ketoconazole, loratadine, menadione, norharmane and raloxifene) whose structures are shown in Fig. 4. To calculate the $IC_{50}$ values for the three AOX isoforms, the S9 fraction of HEK293 cells were co-incubated with five different concentrations of each putative inhibitor and phthalazine. The $IC_{50}$ values determined are shown in Table 2. Regardless of the AOX enzyme considered, clozapine and ketoconazole were devoid of any inhibitory activity at the concentrations considered, which did not allow calculation of reliable $IC_{50}$ values. The inhibitory activity of hydralazine could not be determined because of interference with the AOX derived phthalazone product. Amitriptyline and chlorpromazine showed inhibitory

effects on the three AOX enzymes. However, the $IC_{50}$ values of both compounds for human and mouse AOX1 were slightly lower than the corresponding values determined for mouse AOX3. In terms of AOX enzyme specificity, the most interesting drugs were raloxifene, 17β-estradiol, menadione and norharmane. Raloxifene and 17β-estradiol exhibited a selective inhibitory effect on human AOX1, with $IC_{50}$ values of 0.06 and 1.44 μM, respectively. By converse, menadione and norharmane exerted specific inhibitory effects on mouse AOX3 with $IC_{50}$ values of 0.06 and 0.66 μM, respectively. Fig. 5 contains the scatter plots of the calculated $IC_{50}$ values for human AOX1 vs. mouse AOX1, human AOX1 vs. mouse AOX3 and mouse AOX1 vs. mouse AOX3. The data emphasize the AOX enzyme selectivity of 17β-estradiol, menadione, norharmane and raloxifene (Fig. 5).

### *3.3. Comparison of the inhibitory effects on AOX activity using $O^6$-benzylguanine and phthalazine as substrates*

The effect exerted by AOX inhibitors is dependent on the substrate used as a probe [31]. For this reason, we evaluated the inhibitory activity of the same 10 compounds described above on human and mouse AOX1 using the $O^6$-benzylguanine substrate. The $IC_{50}$ values determined for the 10 inhibitors are shown in Table 2. Fig. 6 contains the scatter plots of the calculated $IC_{50}$ values for human AOX1 vs. mouse AOX1. Except for hydralazine, which inhibited human AOX1 specifically, all the other compounds exerted a similar

inhibitory action on both human and mouse AOX1. The scatter plots contained in Fig. 7 illustrate the correlations between the $IC_{50}$ values calculated with $O^6$-benzylguanine and phthalazine as substrates for both human and mouse AOX1. As for mouse AOX1, the inhibitory effect of menadione was much stronger in the presence of phthalazine than $O^6$-benzylguanine. The calculated $IC_{50}$ values of 17β-estradiol, menadione and raloxifene for the inhibitory action on human AOX1 were significantly lower in the presence of phthalazine than $O^6$-benzylguanine. The results demonstrate substrate- and enzyme-dependent differences in the action of some of the inhibitors considered. In particular, the data indicate that some of the compounds tested represent useful tools to inhibit human AOX1 or mouse AOX3 specifically.

### *3.4. Comparison of the minimum binding energy of six representative inhibitors to human AOX1 and mouse AOX3*

To obtain a deeper understanding of the mode of interaction between human AOX1 or mouse AOX3 and the inhibitors taken into consideration, we conducted an *in silico* docking study using Autodock, a simulation software. Human AOX1 and mouse AOX3 were chosen as target proteins, since the crystal structures of the two enzymes are known (PDB ID: 4UHW, 2.6 Å resolution; 3ZYV, 2.55 Å resolution) [26,27,32]. The minimum binding energies (MBE) of the six compounds which exerted relatively strong inhibitory effects on

the two AOX enzymes are listed in Table 3. The MBE values calculated for 17β-estradiol and raloxifene were lower in the case of human AOX1 than mouse AOX3. By converse, norharmane exhibited higher MBE values with human AOX1 than mouse AOX3. The MBE values of amitriptyline, chlorpromazine and menadione did not differ between the two isoforms. In cases other than menadione, the *in silico* data supported the experimental results obtained *in vitro*.

### *3.5. DDI studies in chimeric mice bearing humanized livers*

We performed studies on the pharmacokinetics of $O^6$-benzylguanine and its AOX-derived metabolite, 8-oxo-$O^6$-benzylguanine in humanized chimeric mice engineered to contain livers with approximately 95.4 ± 4.01% (mean ± SD) human hepatocytes [29]. For these experiments, a group of mice was pretreated with hydralazine to inhibit human AOX1. The plasma concentrations, the $AUC_{0\text{-}24}$, $C_{max}$ and $t_{max}$ of $O^6$-benzylguanine and 8-oxo-$O^6$-benzylguanine and hydralazine after administration of $O^6$-benzylguanine with or without pretreatment of hydralazine, are shown in Fig. 8 and Table 4.

In both groups, $O^6$-benzylguanine was rapidly absorbed with a $t_{max}$ less than 1 h; in the control group, the $C_{max}$ was 1.23 μg/mL, whereas in the pretreatment group, the $C_{max}$ was 5.17 μg/mL. The calculated $AUC_{0\text{–}24}$ in the control group was 2.68 μg/mL·h, whereas the $AUC_{0\text{–}24}$ in the pretreatment group was 40.4 μg/mL·h (Fig. 8, Table 4). These data indicate

that pretreatment of hydralazine led to a significant increase in the exposure of $O^6$-benzylguanine to chimeric mice with humanized livers, consistent with our *in vitro* experimental profile (Table 1,2). For 8-oxo-$O^6$-benzylguanine, an AOX-dependent metabolite, the $C_{max}$ and $AUC_{0-24}$ were similar in both groups (Table 4). However, the plasma concentration of 8-oxo-$O^6$-benzylguanine in the pretreatment group tended to decrease until 3 h after dosing with $O^6$-benzylguanine, when the concentration of hydralazine was high (Fig. 8). This is reflected by the delayed $t_{max}$ of 8-oxo-$O^6$-benzylguanine in the pretreatment group ($t_{max}$ = 10.0 h) compared with that in the control group ($t_{max}$ = 2.33 h) (Table 4). These data indicate that hydralazine suppressed the formation of 8-oxo-$O^6$-benzylguanine when the concentration of hydralazine was high.

## 3. Discussion

Human liver AOX1 plays an important and emerging role in drug metabolism [6–8] and it is likely to be of relevance also in the context of DDI. However, the later aspect is largely overlooked and it has never been the object of specific studies. The involvement of human AOX1 in DDI is likely to be significant in the clinical setting, as numerous putative substrates and inhibitors of the enzyme have been identified [1,16]. Pre-clinical DDI studies involving AOX1 ultimately require *in vivo* approaches which are complicated by the fact that the complement of human and mouse liver AOXs is different [10]. Human hepatocytes are

characterized by the expression of a single enzyme, AOX1, while the mouse counterparts express the putative AOX1 orthologous protein and much higher amounts of a different isoenzyme known as AOX3 [13]. While the substrate-binding regions of human and mouse AOX1 are characterized by a high level of primary structure similarity (84%), this similarity decreases to 61% if human and mouse AOX1 are compared with mouse AOX3. Thus, it is important to define whether the three enzymes are endowed with common and/or specific properties in terms of substrate and/or inhibitor specificities. The present study provides initial evidence on the profiles of substrate/inhibitor selectivity of human AOX1, mouse AOX1 and mouse AOX3. To this purpose, we developed models for the independent over-expression of the catalytically active forms of the three native enzymes. We profiled these enzymes for their response to selected inhibitors and two widely used substrates. We tested the relevance of the findings for *in vivo* DDI, with the use of a humanized mouse model [29] following co-administration of the substrate, $O^6$-benzylguanine and the inhibitor, hydralazine.

As for the *in vitro* studies on the metabolic activity of human/mouse AOX1 and mouse AOX3, the two selected substrates, phthalazine and $O^6$-benzylguanine, present isoform-dependent differences. In the case of phthalazine, mouse AOX3 exhibits the highest activity followed by human AOX1 and mouse AOX1. Given the high levels of AOX3 expression in mouse liver, it is likely that AOX-dependent phthalazine metabolic activity is

higher in mouse than human liver. In the presence of $O^6$-benzylguanine, human AOX1 exhibits a much higher activity than mouse AOX1, while mouse AOX3 does not recognize the substrate. These data suggest that AOX-dependent $O^6$-benzylguanine metabolic activity is remarkably higher in human liver than the mouse counterpart.

Some of the AOX inhibitors tested in this study are characterized by selectivity for one of the human or mouse AOXs expressed in the corresponding liver tissue. The rank order of $IC_{50}$ values for human AOX1 approximately reflected the $IC_{50}$ values obtained for human liver cytosol by Obach et al. (2004) [16]; however, the absolute values differed. Furthermore, 17β-estradiol and raloxifene showed selective inhibitory action on human AOX1, whereas menadione and norharmane were specific inhibitors of mouse AOX3. The observations are partly reflected in the work of Sahi et al. (2008) [14] using cytosolic fractions of mouse and human liver, although the substrate is vanillin. In addition, hydralazine showed approximately 50-fold higher inhibitory action on human AOX1 than on mouse AOX1. These results demonstrate enzyme-dependent differences in the action of several inhibitors, particularly in human AOX1 or mouse AOX3.

The action of inhibitors on drug-metabolizing enzymes is modulated by the substrate used as a probe. Substrate-dependent differences have been reported for inhibitors of cytochrome P450 isoforms 3A4 [33,34], 2C9 [35] and 2C19 [36]. As the issue may have implications for drug interactions mediated by AOXs, we addressed the point by comparing

the effects of selected inhibitors on human liver AOX1 and mouse liver AOX1, using the two substrates, phthalazine and $O^6$-benzylguanine. The approach resulted in the definition of substrate- and enzyme-dependent differences in the observed inhibitory effects. In fact, menadione is characterized by a stronger inhibitory action on mouse AOX1, when enzymatic activity is measured with phthalazine rather than $O^6$-benzylguanine. As for human AOX1, 17β-estradiol, menadione and raloxifene exhibit a stronger inhibitory effect in the presence of phthalazine than $O^6$-benzylguanine. In line with some of these data, a recent report describes substrate-dependent differences in the action exerted by seven inhibitors on human liver AOX1 [31]. The two substrates used in this study are phthalazine and N-[(2-dimethylamino)ethyl]acridine-4-carboxamide (DACA), which is a much bulkier molecule. In this report, DACA exhibits a decrease in the inhibitory effect of the seven tested inhibitors, with a shift of the inhibition mode from competitive to uncompetitive. It is possible that the differences observed are attributable to the different molecular size of phthalazine and DACA. In fact, an uncompetitive mode of action is indicative of the affinity by which the inhibitor binds to the substrate–enzyme complex [31]. As $O^6$-benzylguanine is a bulkier molecule than phthalazine, our findings may also have a similar explanation. In this study, the comparison was performed between only two substrates. Further experiments using several substrates are required to understand the inhibitory effects in a substrate-dependent manner and their detailed mechanisms of action.

In this context, the availability of the crystal structures of human AOX1 and mouse AOX3 allowed us to perform docking studies aimed at getting deeper insights into the mode of interaction between the two enzymes and the selected inhibitors. These computational analyses permitted the calculation of the MBEs for six common inhibitors of human AOX1 and mouse AOX3. The observation that the MBE rank order reflects the $IC_{50}$ values determined with our *in vitro* study is consistent with the idea that the selected inhibitors bind to the active site of the two liver AOX enzymes. However, it should be emphasized that menadione represented an exception to the rule because the MBE was similar between human AOX1 and mouse AOX1. Considering a previous report suggesting that menadione binds to the FAD binding site rather than the active site of AOX [37], the discrepancy between the *in silico* and *in vitro* results for menadione may be because of the property that this compound binds to a site other than the active site of AOX.

In order to investigate the relevance of our *in vitro* models for *in vivo* DDI via inhibition of AOX1-dependent metabolism, we performed PK studies in a humanized mouse model. For this type of study, we selected the human AOX1 substrate, $O^6$-benzylguanine, and the corresponding inhibitor, hydralazine [18]. Exposure to hydralazine would be sufficient to cause inhibition of human AOX1, considering the $IC_{50}$ value in human AOX1 and plasma unbound fraction (fu, 0.12) of hydralazine in humans [38]; however, the fu values in chimeric mice with humanized liver were assumed to be similar to those in humans because human

albumin is expressed in the blood of chimeric mice with humanized liver.

As expected, inhibition of human AOX1 by hydralazine significantly increased the $C_{max}$ and $AUC_{0-24}$ values of $O^6$-benzylguanine. However, these results cannot be completely explained by hydralazine dependent inhibition of AOX. In fact, the $AUC_{0-24}$ and $C_{max}$ of 8-oxo-$O^6$-benzylguanine were similar between groups regardless of hydralazine pretreatment. As the formation of 8-oxo-$O^6$-benzylguanine tended to decrease with high plasma concentrations of hydralazine, it is likely that hydralazine partly contributed to the increase in plasma levels of $O^6$-benzylguanine. These results indicate that AOX inhibition causes DDI effects *in vivo*. However, the possibility that strong AOX inhibitory drugs other than hydralazine (e.g., raloxifene) induce DDI should be investigated.

It should be noted the possibility that the contribution exerted by the residual mouse hepatocytes may present in the liver of our humanized animals. However, the influence of residual mouse hepatocytes is likely to be negligible in our experimental condition, as human AOX1 oxidizes $O^6$-benzylguanine much more extensively and efficiently than mouse AOX1 and AOX3.

In summary, this study provides evidence that substrates undergo metabolism in an isoform-dependent manner, and some established AOX inhibitors exhibit differential action depending on the AOX enzyme and the substrate considered. In addition, our results imply that caution should be taken when selecting the animal species to be used for pre-clinical

safety studies and AOX-dependent DDI studies.

## Declaration of interest

Sanoh and Ohta received financial support from PhoenixBio Co., Ltd in collaboration study. Sugahara, Yanagi, Ishida and Tateno are employees of PhoenixBio co., Ltd..

## Acknowledgement

This research was supported by Phoenix Biotechnology Co., Ltd.

## Author Contribution

*Participated in research design*: Sanoh, Kotake, Tateno, Tayama, Sugihara, Kitamura, Terao, Garattini and Ohta.

*Conducted experiments*: Takaoka, Sanoh, Okuda, Sugahara, Yanagi, Ishida, Kurosaki and Terao.

*Contributed new reagents or analytic tools*: Sugahara, Yanagi, Ishida, Tateno, Kurosaki, Terao and Garattini.

*Performed data and analysis*: Takaoka and Okuda.

*Wrote or contributed to the writing of the manuscript*: Takaoka, Sanoh, Terao and Garattini.

## References

[1] S. Kitamura, K. Sugihara, S. Ohta, Drug-metabolizing ability of molybdenum hydroxylases, Drug Metab. Pharmacokinet. 21 (2006) 83–98. doi:10.2133/dmpk.21.83.

[2] E. Garattini, M. Fratelli, M. Terao, Mammalian aldehyde oxidases: Genetics, evolution and biochemistry, Cell. Mol. Life Sci. 65 (2008) 1019–1048. doi:10.1007/s00018-007-7398-y.

[3] N.A. Meanwell, Improving Drug Candidates by Design : A Focus on Physicochemical Properties As a Means of Improving Compound Disposition and Safety, Chem Res Toxicol. 24 (2011) 1420–1456. doi:10.1021/tx200211v.

[4] N.A. Meanwell, Synopsis of some recent tactical application of bioisosteres in drug design, J Med Chem. 54 (2011) 2529–2591. doi:10.1021/jm1013693.

[5] D.J.S. Jean, C. Fotsch, Mitigating Heterocycle Metabolism in Drug Discovery, J Med Chem. 55 (2012) 6002–6020. doi:10.1021/jm300343m.

[6] E. Garattini, M. Terao, Aldehyde oxidase and its importance in novel drug discovery: present and future challenges, Expert Opin. Drug Discov. 8 (2013) 641–54. doi:10.1517/17460441.2013.788497.

[7] J.M. Hutzler, R.S. Obach, D. Dalvie, M. a Zientek, Strategies for a comprehensive understanding of metabolism by aldehyde oxidase, Expert Opin. Drug Metab. Toxicol. 9 (2013) 153–68. doi:10.1517/17425255.2013.738668.

[8] D.C. Pryde, D. Dalvie, Q. Hu, P. Jones, R.S. Obach, T.D. Tran, Aldehyde oxidase: An enzyme of emerging importance in drug discovery, J. Med. Chem. 53 (2010) 8441–8460. doi:10.1021/jm100888d.

[9] S. Sanoh, Y. Tayama, K. Sugihara, S. Kitamura, Drug Metabolism and Pharmacokinetics Significance of aldehyde oxidase during drug development: Effects on drug metabolism, pharmacokinetics, toxicity, and efficacy, Drug Metab Pharmacokinet. 30 (2015) 52–63. doi:10.1016/j.dmpk.2014.10.009.

[10] E. Garattini, M. Terao, The role of aldehyde oxidase in drug metabolism, Expert Opin. Drug Metab. Toxicol. 8 (2012) 487–503. doi:10.1517/17425255.2012.663352.

[11] M. Kurosaki, M. Bolis, M. Fratelli, M.M. Barzago, L. Pattini, G. Perretta, M. Terao, E. Garattini, Structure and evolution of vertebrate aldehyde oxidases: From gene duplication to gene suppression, Cell. Mol. Life Sci. 70 (2013) 1807–1830. doi:10.1007/s00018-012-1229-5.

[12] M. Terao, M.J. Romao, S. Leimkuhler, M. Bolis, M. Fratelli, C. Coelho, T. Santos-Silva, E. Garattini, Structure and function of mammalian aldehyde oxidases, Arch Toxicol. 90 (2016) 753–780. doi:10.1007/s00204-016-1683-1.

[13] R. Vila, M. Kurosaki, M.M. Barzago, M. Kolek, A. Bastone, L. Colombo, M. Salmona, M. Terao, E. Garattini, Regulation and biochemistry of mouse molybdo-flavoenzymes: The DBA/2 mouse is selectively deficient in the expression of aldehyde oxidase

homologues 1 and 2 and represents a unique source for the purification and characterization of aldehyde oxidase, J. Biol. Chem. 279 (2004) 8668–8683. doi:10.1074/jbc.M308137200.

[14] J. Sahi, K. Kahn, C. Black, Aldehyde Oxidase Activity and Inhibition in Hepatocytes and Cytosolic Fraction from Mouse, Rat,Monkey and Human, Drug Metab. Lett. 2 (2008) 176–83. doi:10.2174/187231208785425818.

[15] K.G. Jensen, A.-M. Jacobsen, C. Bundgaard, D.O. Nilausen, Z. Thale, G. Chandrasena, M. Jorgensen, Lack of Exposure in a First-in-Man Study Due to Aldehyde Oxidase Metabolism: Investigated by Use of 14C-microdose, Humanized Mice, Monkey Pharmacokinetics, and In Vitro Methods, Drug Metab. Dispos. 45 (2016) 68–75. doi:10.1124/dmd.116.072793.

[16] R.S. Obach, P. Huynh, M.C. Allen, C. Beedham, Human liver aldehyde oxidase: inhibition by 239 drugs, J. Clin. Pharmacol. 44 (2004) 7–19. doi:10.1177/0091270003260336.

[17] C. Johnson, C. Stubley-Beedham, J.G. Stell, Hydralazine: a potent inhibitor of aldehyde oxidase activity in vitro and in vivo, Biochem. Pharmacol. 34 (1985) 4251–6.

[18] T.J. Strelevitz, C.C. Orozco, R.S. Obach, Hydralazine as a selective probe inactivator of aldehyde oxidase in human hepatocytes: Estimation of the contribution of aldehyde oxidase to metabolic clearance, Drug Metab. Dispos. 40 (2012) 1441–1448.

doi:10.1124/dmd.112.045195.

[19] D.J. Critchley, D.J. Rance, C. Beedham, Biotransformation of carbazeran in guinea pig: effect of hydralazine pretreatment, Xenobiotica. 24 (1994) 37–47. doi:10.3109/00498259409043219.

[20] Y. Tayama, K. Sugihara, S. Sanoh, K. Miyake, S. Morita, S. Kitamura, S. Ohta, Effect of tea beverages on aldehyde oxidase activity, Drug Metab. Pharmacokinet. 26 (2011) 94–101. doi:10.2133/dmpk.DMPK-10-NT-078.

[21] J.T. Barr, J.P. Jones, N.H. Oberlies, M.F. Paine, Inhibition of human aldehyde oxidase activity by diet-derived constituents: Structural influence, enzyme-ligand interactions, and clinical relevance, Drug Metab. Dispos. 43 (2015) 34–41. doi:10.1124/dmd.114.061192.

[22] S. Kitamura, K. Nitta, C. Tanoue, K. Sugihara, T. Inoue, T. Horie, S. Ohta, Aldehyde Oxidase-Catalyzed Metabolism of N1-Methylnicotinamide in Vivo and in Vitro in Chimeric Mice with Humanized Liver, Drug Metab Dispos. 36 (2008) 1202–1205. doi:10.1124/dmd.107.019075.

[23] S. Sanoh, A. Horiguchi, K. Sugihara, Y. Kotake, Y. Tayama, H. Ohshita, C. Tateno, T. Horie, S. Kitamura, S. Ohta, Prediction of in vivo hepatic clearance and half-life of drug candidates in human using chimeric mice with humanized liver, Drug Metab. Dispos. 40 (2012) 322–328. doi:10.1124/dmd.111.040923.

[24] S. Sanoh, K. Nozaki, H. Murai, S. Terashita, T. Teramura, S. Ohta, Prediction of human metabolism of FK3453 by aldehyde oxidase using chimeric mice transplanted with human or rat hepatocytes, Drug Metab. Dispos. 40 (2012) 76–82. doi:10.1124/dmd.111.041954.

[25] M. Terao, M. Kurosaki, M. Marini, M.A. Vanoni, G. Saltini, V. Bonetto, A. Bastone, C. Federico, S. Saccone, R. Fanelli, M. Salmona, E. Garattini, Purification of the Aldehyde Oxidase homolog 1 (AOH1) protein and cloning of the AOH1 and aldehyde oxidase homolog 2 (AOH2) genes: Identification of a novel molybdo-flavoprotein gene cluster on mouse chromosome 1, J. Biol. Chem. 276 (2001) 46347–46363. doi:10.1074/jbc.M105744200.

[26] C. Coelho, M. Mahro, J. Trincão, A.T.P. Carvalho, M.J. Ramos, M. Terao, E. Garattini, S. Leimkühler, M.J. Romão, The first mammalian aldehyde oxidase crystal structure: Insights into substrate specificity, J. Biol. Chem. 287 (2012) 40690–40702. doi:10.1074/jbc.M112.390419.

[27] C. Coelho, A. Foti, T. Hartmann, T. Santos-Silva, S. Leimkühler, M.J. Romão, Structural insights into xenobiotic and inhibitor binding to human aldehyde oxidase, Nat. Chem. Biol. 11 (2015) 779–85. doi:10.1038/nchembio.1895.

[28] G. Morris, R. Huey, W. Lindstrom, M. Sanner, R. Belew, D. Goodsell, A. Olson, AutoDock4 and AutoTools4: Automated docking with selective receptor, J Comput

Chem. 16 (2009) 2785–91. doi:10.1002/jcc.21256.

[29] C. Tateno, Y. Kawase, Y. Tobita, S. Hamamura, H. Ohshita, H. Yokomichi, H. Sanada, M. Kakuni, A. Shiota, Y. Kojima, Y. Ishida, H. Shitara, N.A. Wada, H. Tateishi, M. Sudoh, S.I. Nagatsuka, K.I. Jishage, M. Kohara, Generation of novel Chimeric mice with humanized livers by using hemizygous cDNA-uPA/SCID mice, PLoS One. 10 (2015) 1–20. doi:10.1371/journal.pone.0142145.

[30] G.I. Panoutsopoulos, C. Beedham, Enzymatic oxidation of phthalazine with guinea pig liver aldehyde oxidase and liver slices: Inhibition by isovanillin, Acta Biochim. Pol. 51 (2004) 943–951. doi:045104943.

[31] J.T. Barr, J.P. Jones, Evidence for substrate-dependent inhibition profiles for human liver aldehyde oxidase, Drug Metab. Dispos. 41 (2013) 24–29. doi:10.1124/dmd.112.048546.

[32] M. Mahro, C. Coelho, J. Trincao, D. Rodrigues, M. Terao, E. Garattini, M. Saggu, F. Lendzian, P. Hildebrandt, M.J. Romao, S. Leimkuehler, Characterization and crystallization of mouse aldehyde oxidase 3 (mAOX3): from mouse liver to Escherichia coli heterologous protein expression, Drug Metab. Dispos. 39 (2011) 1939–1945. doi:10.1124/dmd.111.040873.

[33] K.E. Kenworthy, J.C. Bloomer, S.E. Clarke, J.B. Houston, CYP3A4 drug interactions: Correlation of 10 in vitro probe substrates, Br. J. Clin. Pharmacol. 48 (1999) 716–727.

doi:10.1046/j.1365-2125.1999.00073.x.

[34] R.S. Foti, D.A. Rock, L.C. Wienkers, J.L. Wahlstrom, Selection of alternative CYP3A4 probe substrates for clinical drug interaction studies using in vitro data and in vivo simulation, Drug Metab. Dispos. 38 (2010) 981–987. doi:10.1124/dmd.110.032094.

[35] V. Kumar, J.L. Wahlstrom, D.A. Rock, C.J. Warren, L.A. Gorman, T.S. Tracy, CYP2C9 inhibition: Impact of probe selection and pharmacogenetics on in vitro inhibition profiles, Drug Metab. Dispos. 34 (2006) 1966–1975. doi:10.1124/dmd.106.010926.

[36] R.S. Foti, J.L. Wahlstrom, CYP2C19 inhibition: The impact of substrate probe selection on in vitro inhibition profiles, Drug Metab. Dispos. 36 (2008) 523–528. doi:10.1124/dmd.107.019265.

[37] M. Siah, M.H. Farzaei, M.R. Ashrafi-Kooshk, H. Adibi, S.S. Arab, M.R. Rashidi, R. Khodarahmi, Inhibition of Guinea pig aldehyde oxidase activity by different flavonoid compounds: An in vitro study, Bioorg. Chem. 64 (2016) 74–84. doi:10.1016/j.bioorg.2015.12.004.

[38] R.S. Obach, F. Lombardo, N.J. Waters, Trend Analysis of a Database of Intravenous Pharmacokinetic Parameter in Humans for 670 Drug Compounds., Drug Metab Dispos. 36 (2008) 1385–1405. doi:10.1124/dmd.108.020479.

## Figure legends

**Fig. 1.** *Characterization of the HEK-293 derived cell lines over-expressing human AOX1, mouse AOX1 and mouse AOX3* HEK293 derived cell lines stably transfected with human *AOX1*, mouse *AOX1* and mouse *AOX3* were grown in the absence or presence of tetracycline (1 µg/ml, TET) for 48 hours. (**A**) The Western blot analysis illustrate the expression of human AOX1, mouse AOX1 and mouse AOX3 proteins. Cytosolic extracts containing 20 µg of protein/lane were used. (**B**) Human AOX1, mouse AOX1 and mouse AOX3 enzymatic activities were determined using the Amplex red assay in the presence of 30 µg of cytosolic protein extract and phthalazine (1 mM) as a substrate.

**Fig. 2.** *Chemical structures of phthalazine, $O^6$-benzylguanine and corresponding AOX-dependent oxidation products*

**Fig. 3.** *Enzyme kinetics of phthalazine and $O^6$-benzylguanine oxidation in the S9 fraction obtained from AOX overexpressing HEK293 cell lines*. The enzymatic activities are presented as the mean ± S.D. of 3 replicates. These data were fitted to the Michaelis–Menten equation using GraphPad Prism.

**Fig. 4.** *Chemical structures of the model inhibitors used in the study*

**Fig. 5.** *Correlations between the $IC_{50}$ values of selected AOX inhibitors measured for couples of AOX enzymes* The indicated enzymes were exposed to selected AOX inhibitors and enzyme activity was determined using phthalazine as the substrate. The $IC_{50}$ values (µM) calculated for each inhibitor on the indicated couples of AOX enzymes were plotted. In each plot, only the inhibitors showing specificity for one of the AOX enzymes are indicated. The maximum concentrations of inhibitors were used when the $IC_{50}$ values could not be determined.

**Fig. 6.** *Correlations between the $IC_{50}$ values of selected AOX inhibitors measured for the human and mouse AOX1 couple* Human and mouse AOX1 were exposed to selected AOX inhibitors and enzyme activity was determined using $O^6$-benzylguanine as the substrate. The $IC_{50}$ values (µM) calculated for each inhibitor on the indicated couples of AOX enzymes were plotted. In each plot, only hydralazine, showing specificity for human AOX1 is indicated. The maximum concentrations of inhibitors were used when the $IC_{50}$ values could not be determined.

**Fig. 7.** *Correlations between the $IC_{50}$ values of selected AOX inhibitors using phthalazine and $O^6$-benzylguanine as substrates* Human and mouse AOX1 were exposed to selected AOX inhibitors and enzyme activity was determined using phthalazine and $O^6$-benzylguanine as substrates. The $IC_{50}$ values (μM) calculated for each inhibitor using the indicated substrates were plotted. In each plot, only the inhibitors showing specificity with one of the two substrates are indicated. The maximum concentrations of inhibitors were used when the $IC_{50}$ values could not be determined.

**Fig. 8.** *$O^6$-benzylguanine and 8-oxo-$O^6$-benzylguanine concentrations in the plasma of humanized mice* Chimeric mice were orally administered $O^6$-benzylguanine (10 mg/kg) with or without pretreatmet of hydralazine (30 mg/kg) as indicated: the plasma concentrations of $O^6$-benzylguanine, 8-oxo-$O^6$-benzylguanine and hydralazine are illustrated in the graphs. Each value is the mean ± S.D of 3 independent animals

Fig.1

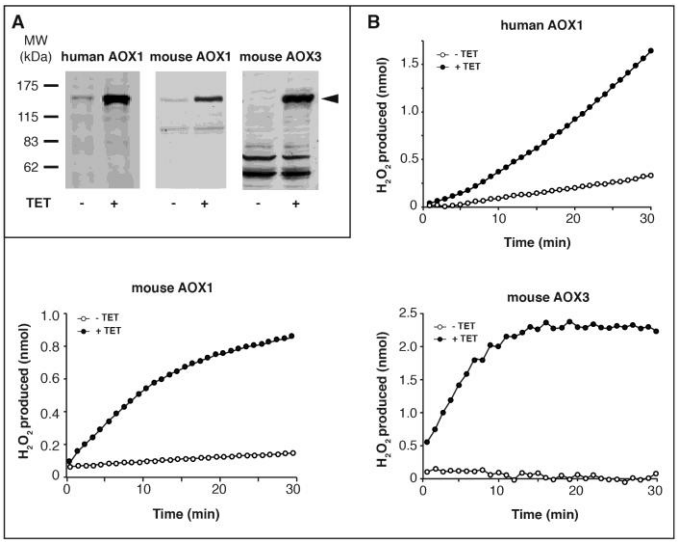


1
2

Fig.2

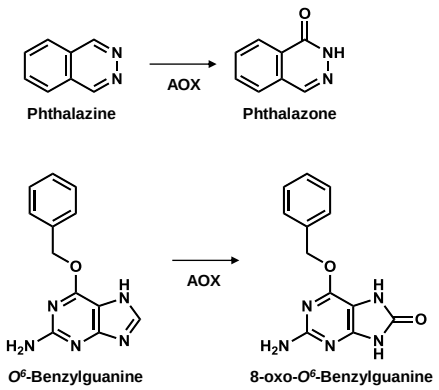


1
2

Fig.3

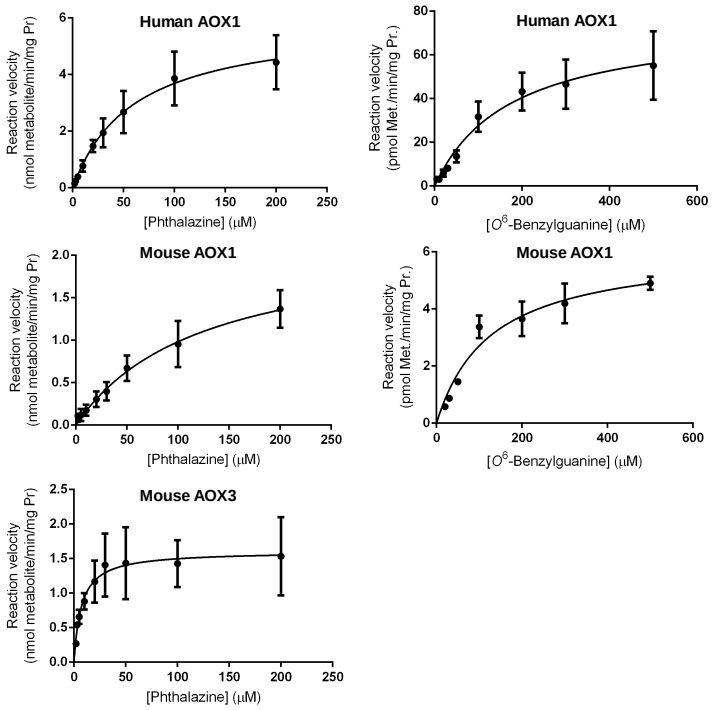


1
2

Fig.4

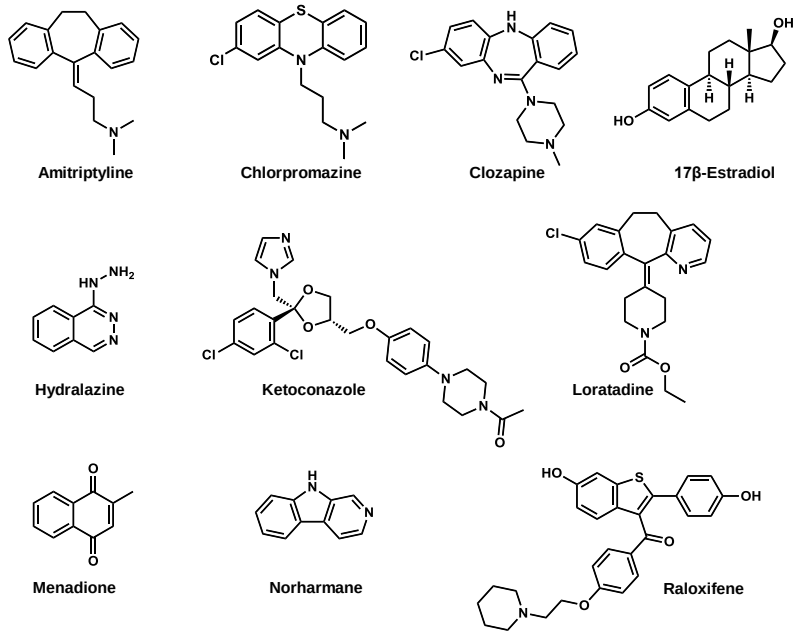


1
2

Fig.5

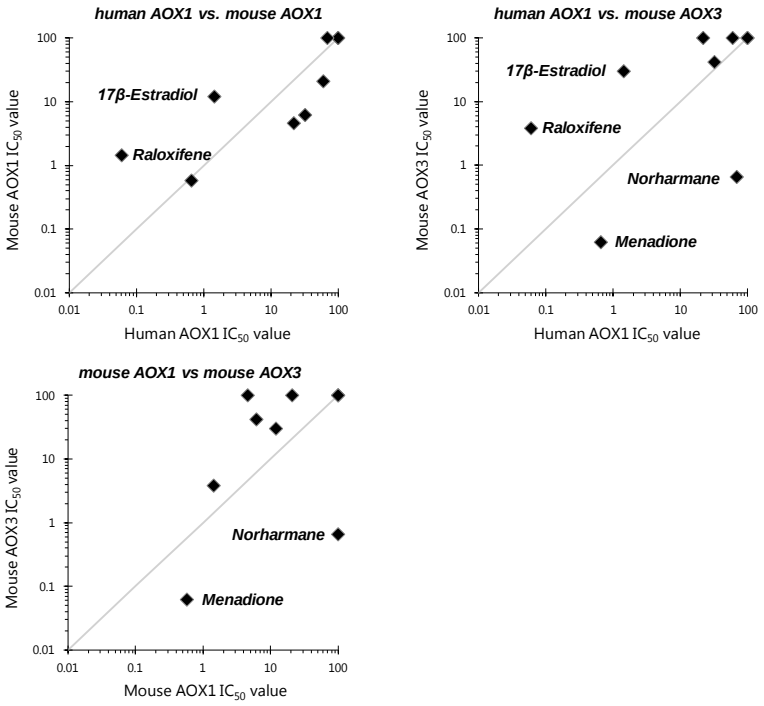


1
2

Fig.6

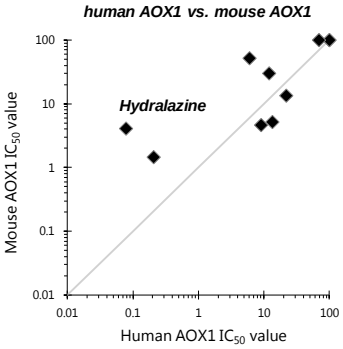


1
2

Fig.7

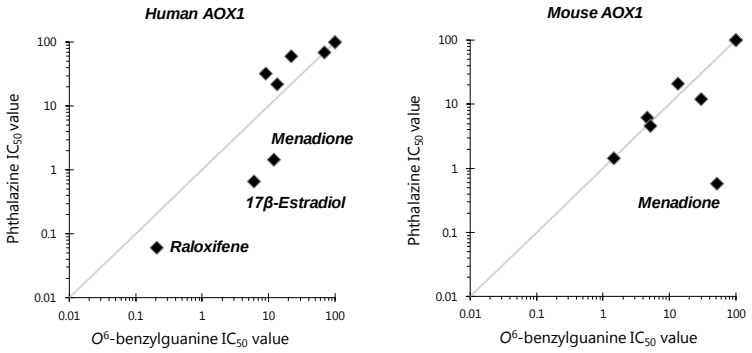


1
2

Fig.8

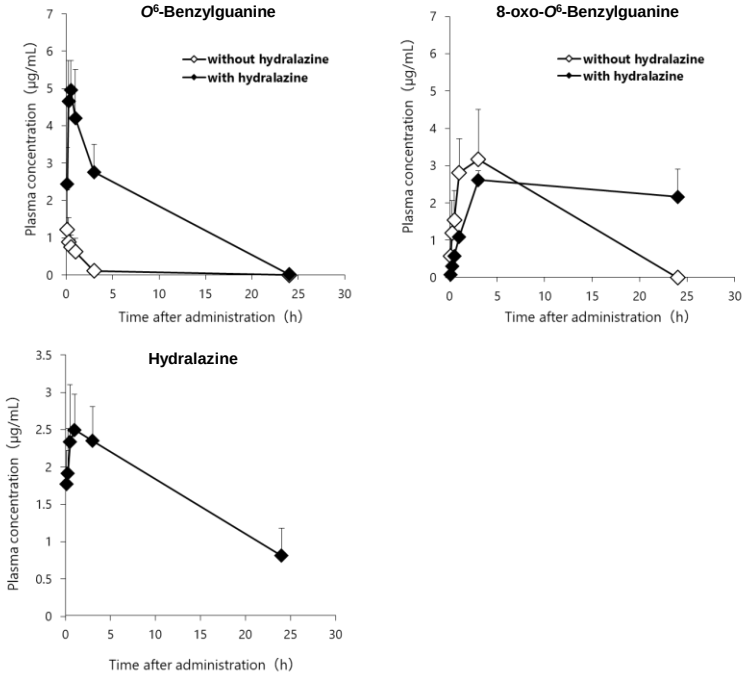


1
2

Table 1

Enzyme kinetic parameters for AO isozyme-catelyzed oxidation in S9 from each HEK293.

| | phthalazine | | $O^6$-benzylguanine | |
|---|---|---|---|---|
| Isoenzyme | $K_m$ (μM) | $V_{max}$ (nmol/min/mg) | $K_m$ (μM) | $V_{max}$ (pmol/min/mg) |
| human AOX1 | 60.2 ± 13.3 | 5.91 ± 0.56 | 175 ± 48.6 | 75.8 ± 8.98 |
| mouse AOX1 | 123 ± 32.3 | 2.19 ± 0.30 | 126 ± 27.8 | 6.13 ± 0.51 |
| mouse AOX3 | 7.18 ± 2.15 | 1.61 ± 0.12 | ND[a] | ND[a] |

All values are expressed as mean ± S.E.M. of 3. replicates.

a : kinetic parameters could not be determined because formed metabolite was not detected.

1

2

Table 2

$IC_{50}$ values (μM) of ten compounds for oxidation of phthalazine and $O^6$-benzylguanine catalyzed by three AOX isozymes.

| Compounds | phthalazine | | | $O^6$-benzylguanine | |
|---|---|---|---|---|---|
| | human AOX1 | mouse AOX1 | mouse AOX3 | human AOX1 | mouse AOX1 |
| Amitriptyline | 60.3 ± 4.63 | 20.9 ± 0.63 | >100[a] | 21.9 ± 0.89 | 13.4 ± 0.38 |
| Chlorpromazine | 32.3 ± 2.16 | 6.17 ± 0.30 | 41.8 ± 2.30 | 9.06 ± 0.64 | 4.64 ± 0.23 |
| Clozapine | >100[a] | >100[a] | >100[a] | >100[a] | >100[a] |
| 17β-Estradiol | 1.44 ± 0.04 | 12.0 ± 0.96 | >30[a] | 12.0 ± 0.77 | >30[a] |
| Hydralazine | NC[b] | NC[b] | NC[b] | 0.08 ± 0.01 | 4.08 ± 0.40 |
| Ketconazole | >100[a] | >100[a] | >100[a] | >100[a] | >100[a] |
| Loratadine | 22.0 ± 0.88 | 4.59 ± 0.19 | >100[a] | 13.5 ± 0.62 | 5.17 ± 0.24 |
| Menadione | 0.66 ± 0.03 | 0.58 ± 0.02 | 0.06 ± 0.01 | 6.03 ± 0.28 | 51.9 ± 9.97 |
| Norharmane | 69.2 ± 7.37 | >100[a] | 0.66 ± 0.02 | 69.4 ± 10.7 | >100[a] |
| Raloxifene | 0.06 ± 0.01 | 1.44 ± 0.07 | 3.81 ± 0.22 | 0.20 ± 0.02 | 1.45 ± 0.03 |

All values are expressed as mean ± S.E.M. of 3 replicates.

a：$IC_{50}$ could not be determined because of ≦50% inhibition on AO activities in the test concentration.

b：$IC_{50}$ could not be calculated because of interference by phthalazone formed from hydralazine in LC/MS/MS.

1

2

Table 3

Minimum binding energy of six compounds against AO isozymes

| | minimum binding energy (kcal/mol) | |
|---|---|---|
| Compounds | human AOX1 | mouse AOX3 |
| Amitriptyline | -6.81 | -7.52 |
| Chlorpromazine | -7.01 | -7.33 |
| 17β-Estradiol | -8.90 | -6.71 |
| Menadione | -6.43 | -6.57 |
| Norharmane | -6.88 | -8.13 |
| Raloxifene | -9.21 | -8.13 |

1

2

Table 4

PK parameter of $O^6$-benzylguanine and 8-oxo-$O^6$-benzylguanine in chimeric mice with humanized livers

after oral administration with 10 mg/kg $O^6$-benzylguanine with or without pretreatment with 30 mg/kg hydralazine.

| | $O^6$-benzylguanine | | | 8-oxo-$O^6$-benzylguanine | | |
|---|---|---|---|---|---|---|
| condition | $C_{max}$ (μg/mL) | $t_{max}$ (h) | $AUC_{0-24}$ (μg/mL・h) | $C_{max}$ (μg/mL) | $t_{max}$ (h) | $AUC_{0-24}$ (μg/mL・h) |
| without hydralazine | 1.23 ± 0.89 | 0.70 ± 0.52 ** | 2.68 ± 1.72 | 3.19 ± 1.30 ** | 2.33 ± 1.15 | 41.1 ± 17.0 |
| with hydralazine | 5.17 ± 0.94 | 0.58 ± 0.38 | 40.4 ± 10.7 | 2.82 ± 0.19 | 10.0 ± 12.1 | 54.5 ± 4.82 |

All values are expressed as mean ± S.D. of 3 replicates.

** $P$< 0.01 compared to without hydralazine

1

2

Graphical Abstract

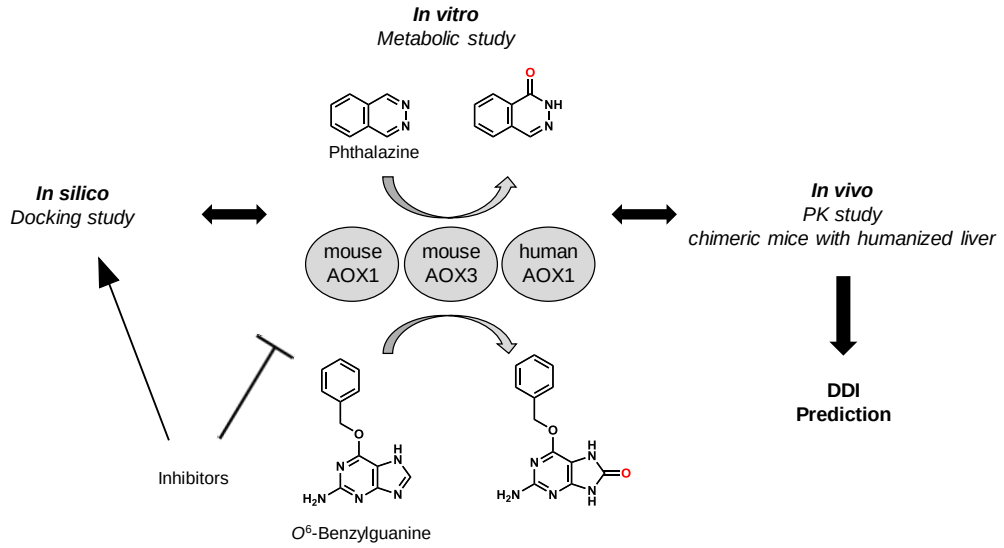


1